RESEARCH ARTICLE

Application of the two-step Lax&Wendroff-FCT and the CE-SE method to flow transport in wall-flow monoliths

J. R. Serrano, F. J. Arnau, P. Piqueras* and O. García-Afonso

Universitat Politècnica de València, CMT-Motores Térmicos, Camino de Vera s/n, 46022
Valencia, Spain.

Gas dynamic codes are computational tools applied to the analysis of air management in internal combustion engines. The governing equations in one-dimensional elements are approached assuming compressible unsteady non-homentropic flow and are commonly solved applying finite difference numerical methods. These techniques can be also applied to the calculation of flow transport in complex systems such as wall-flow monoliths. These elements are characterized by alternatively plugged channels with porous walls. It filters the particulates when the flow goes through the wall from the inlet to the outlet channels. Therefore, this process couples the solution of every pair of inlet and outlet channels. In this study, the adaptation of the two-step Lax&Wendroff method and the CE-SE method is performed to be applied in the solution of flow transport in wall-flow monolith channels. The influence on the prediction ability is analysed by a shock-tube test and experimental data obtained under impulsive flow conditions.

Keywords: Diesel particulate filter; Shock-capturing methods; Lax&Wendroff; CE-SE; FCT

1. Introduction

The need to fulfil the increasingly restrictive emission regulations is leading the automotive industry to adopt the extensive use of aftertreatment systems in internal combustion engines. The development of these systems is conditioned by their effects on engine performance and gas flow path [1, 2], but also by the competitive nature of the market, which demands the manufacturers to provide solutions regarding engine architecture and technology with high timing restrictions.

All these determinants highlight the inclusion of aftertreatment systems into gas dynamic codes. The main objective of this computational tool is the reliable evaluation of the engine performance with low computational cost [18]. Furthermore, studies on isolated engine systems can be performed. Hence the importance of a proper development of fluid dynamic aftertreatment models. In the case of the wall-flow DPF, the models are usually simplified to quasi-steady incompressible flow because of the traditional placement of this element at the engine tailpipe [17]. However, the improvement of the wall-flow DPF modelling regarding aspects such as the prediction of the acoustic response [20], the heat transfer [9] or the evaluation of pre-turbo aftertreatment systems [1, 2] is leading to the consideration of unsteady and compressible flow effect [16, 20].

A wall-flow DPF consists of a ceramic monolith with small axial parallel channels separated by a porous wall. At the inlet cross-section, the channels are alternatively plugged defining the inlet and outlet channels. The flow enters to the

---

*Corresponding author. Email: pedpicab@mot.upv.es

monolith through the inlet channels, which are plugged at its outlet cross-section. As a consequence, the flow inside the inlet channels is forced to flow across the porous substrate walls, where the soot particulates are filtrated and accumulated until the regeneration process takes place. Finally, the clean gas flow leaves the monolith through the outlet channels, which have the outlet cross-section open to the exhaust tailpipe. According to this architecture, the flow inside wall-flow monoliths is modelled as one-dimensional. However, finite difference numerical methods, which are traditionally applied in gas dynamic codes [8, 21] to obtain the numerical solution, need to be adapted. It is due to the flow exiting or entering to the inlet and outlet channels respectively, which means the coupling between the systems of governing equations of both channels.

The method of characteristics (MoC) has been adapted to the solution of the boundary conditions in the inlet and outlet channels of wall-flow monoliths [7]. The present work deals with the solution of the internal nodes in wall-flow monolith channels. The adaptation and evaluation of the two-step Lax&Wendroff method [13] and the CE-SE method [5, 6] to be applied in square channels of wall-flow DPFs is discussed. In the case of the two-step Lax&Wendroff method, the filtration velocity is calculated at the nodes which define the second step, so that simplifications taken in previous works [20] are overcome. Additionally, the flux corrected transport (FCT) technique [3, 4] is considered to be coupled to the two-step Lax&Wendroff method. The influence of the specific formulation of the FCT technique is analysed in order to assess its capability in wall-flow DPF applications to remove the spurious oscillations produced by second order symmetric numerical methods. A shock-tube test affecting the one-dimensional domain of a pair of inlet and outlet channels and an experiment under impulsive flow conditions are proposed to compare the performance of the different numerical methods.

2.   Governing equations in wall-flow DPF channels

Wall-flow diesel particulate filters are the most common type of diesel particulate traps. This typology of filter consists of a monolithic structure characterized by a bundle of small axial parallel channels, typically of square cross-section. Adjacent channels are alternatively plugged at each end, so that the flow inside the inlet channels is forced to flow across the porous substrate walls. The soot particulates are deposited and accumulated inside and on the porous medium until a regeneration event takes place. Finally, the gas flow goes into the outlet channel and leaves the monolith.

According to this flow path, the governing equations in an inlet or outlet channel are represented by equations (1), (4) and (5). These conservation equations are approached assuming the flow inside the monolith channels to be one-dimensional compressible unsteady and non-homentropic and the flow inside the porous medium to have a quasi-steady behaviour. The system is closed with the gas state equations in every channel and the equation governing the pressure drop associated with the flow passage through the porous medium.

- Mass conservation

$$\frac{\partial \rho_k}{\partial t} + \frac{\partial (\rho_k u_k)}{\partial x} + \frac{\rho_k u_k}{F_k}\frac{dF_k}{dx} = (-1)^k \frac{4}{\alpha - 2w_p k}\rho_k u_{w_k} \tag{1}$$

Subscript k takes value 0 or 1 to represent an outlet or inlet channel respectively; ρ is the gas density; u represents the gas velocity; and F is the cross-

section area of the channel. The source term accounts for the mass flow through the porous wall in the inlet or outlet channel. The definition of the source term is sketched in Figure 1, where α defines the honeycomb cell size, which is constant all along the channels, w_p represents the thickness of the particulate layer in the inlet channels and u_w is the filtration velocity, both on the inlet and outlet surfaces of the porous wall.

Assuming negligible the Forchheimer's terms across the porous wall and the particulate layer, the filtration velocity on the inlet surface of the porous wall can be calculated according to the Darcy's law, which couples the governing equations of the inlet and outlet channels [20]:

$$u_{w_1} = \frac{p_1 - p_0}{\frac{\mu_1 w_w}{k_w}\frac{\rho_1(\alpha - 2w_p)}{\rho_0 \alpha} + \frac{\mu_1(\alpha - 2w_p)}{2k_p}\ln\left(\frac{\alpha}{\alpha - 2w_p}\right)} \tag{2}$$

Applying the continuity equation on the porous medium, the filtration velocity on the outlet surface of the porous wall is given by:

$$u_{w_0} = \frac{u_{w_1}\rho_1(\alpha - 2w_p)}{\rho_0 \alpha} \tag{3}$$

- Momentum conservation

$$\frac{\partial(\rho_k u_k)}{\partial t} + \frac{\partial(p_k + \rho_k u_k^2)}{\partial x} + \rho_k \frac{u_k^2}{F_k}\frac{dF_k}{dx} = -\frac{F_w \mu_k u_k}{(\alpha - 2w_p k)^2} \tag{4}$$

In momentum conservation equation, p is the gas pressure, μ is the dynamic viscosity and F_w is the friction loss coefficient for porous wall channels of square cross-section. It is important to note that the transport of momentum perpendicular to the main flow direction is neglected because of the low values of the filtration velocity [20].

- Energy conservation

$$\frac{\partial(e_{0k}\rho_k)}{\partial t} + \frac{\partial(h_{0k}\rho_k u_k)}{\partial x} + h_{0k}\rho_k u_k \frac{1}{F_k}\frac{dF_k}{dx} = q_k \rho_k + (-1)^k \frac{4}{\alpha - 2w_p k}h_{0w}\rho_k u_{w_k} \tag{5}$$

In energy conservation equation, e_0 and h_0 represent the specific stagnation internal energy and enthalpy of the gas respectively, q is the heat per unit of time and area transferred by convection between the gas and the porous wall and h_{0w} is the specific stagnation enthalpy of the flow entering or exiting the porous medium.

3. Numerical solution

The solution of the governing equations is performed by means of shock-capturing finite difference schemes, with the only exception of the boundary conditions, which are solved applying the MoC [7]. The governing equations of a pair of inlet and outlet channels are coupled by the flow across the porous wall, as equation (2) indicates. Therefore, the numerical solvers need to be properly adapted from its traditional formulation for 1D elements with non-porous wall.

3.1   *The two-step Lax&Wendroff method*

The two-step Lax&Wendroff method [13] has been previously adapted to the so-
lution of flow advection in porous wall channels of wall-flow monoliths by Torre-
grosa *et al.* [20] but applying a simplification of the filtration velocity calculation at
the second step. Specifically, two-step Lax&Wendroff method is formulated for the
solution of the governing equations in conservative form [20], which are expressed
in vector form as:

$$\frac{\partial \mathbf{W}_k}{\partial t} + \frac{\partial \mathbf{F}_k}{\partial x} + \mathbf{C}_k + \mathbf{C}_{w_k} = 0 \tag{6}$$

In equation (6), $\mathbf{W}_k$ and $\mathbf{F}_k$ represent the solution and the flux vectors in channel
k respectively. The source terms are divided into two contributions. On the one
hand, the source terms related to the cross-section area change, friction and heat
transfer are included in vector $\mathbf{C}_k$; on the other hand, the source terms character-
istic of the porous medium are arranged in vector $\mathbf{C}_{w_k}$.

The formulation of the two-step Lax&Wendroff method in porous wall channels
is given by equations (7) and (8):

- First step

$$\mathbf{W}_{k,j+\frac{1}{2}}^{n+\frac{1}{2}} = \frac{\mathbf{W}_{k,j}^n + \mathbf{W}_{k,j+1}^n}{2} - \frac{\Delta t}{2\Delta x} \left(\mathbf{F}_{k,j+1}^n - \mathbf{F}_{k,j}^n \right) - \frac{\Delta t}{4} \left(\mathbf{C}_{k,j}^n + \mathbf{C}_{k,j+1}^n \right)$$
$$- \frac{\Delta t}{4} \left(\mathbf{C}_{w_k,j}^n + \mathbf{C}_{w_k,j+1}^n \right) \tag{7}$$

- Second step

$$\mathbf{W}_{k,j}^{n+1} = \mathbf{W}_{k,j}^n - \frac{\Delta t}{\Delta x} \left(\mathbf{F}_{k,j+\frac{1}{2}}^{n+\frac{1}{2}} - \mathbf{F}_{k,j-\frac{1}{2}}^{n+\frac{1}{2}} \right) - \frac{\Delta t}{2} \left(\mathbf{C}_{k,j-\frac{1}{2}}^{n+\frac{1}{2}} + \mathbf{C}_{k,j+\frac{1}{2}}^{n+\frac{1}{2}} \right)$$
$$- \frac{\Delta t}{2} \left(\mathbf{C}_{w_k,j-\frac{1}{2}}^{n+\frac{1}{2}} + \mathbf{C}_{w_k,j+\frac{1}{2}}^{n+\frac{1}{2}} \right) \tag{8}$$

Subscripts j and n in equations (7) and (8) define the space-time mesh identifying
the node (axial position) and the time level respectively.

Figure 2 represents the space-time mesh corresponding to the formulation of the
two-step Lax&Wendroff method given by equations (7) and (8). The solution at
node j and time level $n + 1$ is obtained in two steps. The solution vector in the
first step is calculated at time level $n + \frac{1}{2}$ in the virtual nodes $j - \frac{1}{2}$ and $j + \frac{1}{2}$, so
that the flow entering or exiting the control volume in a time-step is possible to be
determined. According to the definition of the method, this intermediate solution
is obtained from the flow properties calculated at the previous time level (n) at
nodes $j - 1$, j and $j + 1$ but with the inclusion of the porous medium flow terms.
The second-step allows obtaining the flow properties at node j at time level $n + 1$
from the virtual flow at coordinates $(j - \frac{1}{2}, n + \frac{1}{2})$ and $(j + \frac{1}{2}, n + \frac{1}{2})$.

This procedure is applied to nodes in an inlet or outlet channel with a proper
management of the porous medium flow terms. These are dependent on the filtra-
tion velocity, which is calculated at every node and time level n as a function of the
gas pressure in the inlet and outlet channels, the porous medium properties and
the continuity equation applied to the porous wall, as indicated in equations (2)
and (3). In contrast to previous works [7, 20], the source terms related to the porous
medium are obtained in the second step from the solution at time level $n + \frac{1}{2}$ in

nodes $j \pm \frac{1}{2}$.

3.2 *Flux Corrected Transport Technique*

The Flux Corrected Transport (FCT) technique [3, 4] is coupled with the two-step Lax&Wendroff method in order to avoid the spurious oscillations produced by this method in the vicinity of discontinuities. The application of this technique does not require any adaptation when it is applied to the solution of porous wall channels. According to Niessner and Bulaty [15], the FCT technique consists of three steps:

- The first step, which is named *transport*, involves the application of a second order scheme to obtain the solution of the governing equations in the next time level. In this work, this scheme is the two-step Lax&Wendroff method formulated as described in section 3.1.
- The second step involves the application of the diffusion procedure. The solution of the two-step Lax&Wendroff method is post-processed applying an artificial smoothing operator in order to remove non-physical overshoots,

$$D_{k,j}\left(\mathbf{W}_k\right) = \theta\left(\mathbf{W}_{k,j+\frac{1}{2}}\right) - \theta\left(\mathbf{W}_{k,j-\frac{1}{2}}\right) \tag{9}$$

where:

$$\theta\left(\mathbf{W}_{k,j+\frac{1}{2}}\right) = \vartheta\frac{\mathbf{W}_{k,j+1} - \mathbf{W}_{k,j}}{4} \quad \text{and} \quad \theta\left(\mathbf{W}_{k,j-\frac{1}{2}}\right) = \vartheta\frac{\mathbf{W}_{k,j} - \mathbf{W}_{k,j-1}}{4} \tag{10}$$

Depending on the time level in which the smoothing operator is applied, finally it is obtained:

$$\text{Damping} \qquad \bar{\mathbf{W}}_{k,j}^{n+1} = \mathbf{W}_{k,j}^{n+1} + D_{k,j}\left(\mathbf{W}_k^n\right) \tag{11}$$

$$\text{Smoothing} \qquad \bar{\mathbf{W}}_{k,j}^{n+1} = \mathbf{W}_{k,j}^{n+1} + D_{k,j}\left(\mathbf{W}_k^{n+1}\right) \tag{12}$$

The value of ϑ has been set to $\frac{1}{2}$ in order to apply the maximum CFL value fulfilling the TVD property when the FCT is combined with the two-step Lax&Wendroff method [10].

The direct application of this smoothing correction to vector $\mathbf{W_k}$ involves the violation of the conservation equations under non-homentropic flow conditions. Non-constant cross-section 1D elements, which is the case of the inlet channel in loaded DPFs, and mass and enthalpy flow through the porous walls fall into these conditions. Therefore, the smoothing operator is performed on conservative magnitudes instead of components of vector $\mathbf{W_k}$ as proposed by Lie *et al.* [14]. These conservative magnitudes, which will be represented by vector $\mathbf{W}_{c,k}$, are the mass flow, stagnation enthalpy and stagnation pressure.

- The third step of the FCT technique is the application of an anti-diffusion operator. The objective is to recover the second order accuracy in the regions where the solution of the two-step Lax&Wendroff was initially smooth. A non-linear operator is defined as

$$A_{k,j}\left(\mathbf{W}_{c,k}\right) = \Psi\left(\mathbf{W}_{c,k,j-\frac{1}{2}}\right) - \Psi\left(\mathbf{W}_{c,k,j+\frac{1}{2}}\right) \tag{13}$$

where the anti-diffusive operator was defined by Ikeda and Nakagawa [11]

$$\Psi\left(\mathbf{W}_{c,k,j+\frac{1}{2}}\right) = s\max\left[0,\min\left(\frac{5}{8}s\Delta\mathbf{W}_{c,k,j-\frac{1}{2}}, \frac{1}{8}s\left|\Delta\mathbf{W}_{c,k,j+\frac{1}{2}}\right|, \frac{5}{8}s\Delta\mathbf{W}_{c,k,j+\frac{3}{2}}\right)\right] \tag{14}$$

being the terms $s = \text{sign}\left(\Delta\mathbf{W}_{c,k,j+\frac{1}{2}}\right)$ and $\Delta\mathbf{W}_{c,k,j+i} = \mathbf{W}_{c,k,j+i+\frac{1}{2}} - \mathbf{W}_{c,k,j+i-\frac{1}{2}}$.

Depending on the time level in which the correction is applied, the anti-diffusion operator can be written as:

$$\text{Naive} \qquad \bar{\bar{\mathbf{W}}}_{c,k,j}^{n+1} = \bar{\mathbf{W}}_{c,k,j}^{n+1} + A_{k,j}\left(\mathbf{W}_{c,k}^{n}\right) \tag{15}$$

$$\text{Phoenical} \quad \bar{\bar{\mathbf{W}}}_{c,k,j}^{n+1} = \bar{\mathbf{W}}_{c,k,j}^{n+1} + A_{k,j}\left(\mathbf{W}_{c,k}^{n+1}\right) \tag{16}$$

$$\text{Explicit} \qquad \bar{\bar{\mathbf{W}}}_{c,k,j}^{n+1} = \bar{\mathbf{W}}_{c,k,j}^{n+1} + A_{k,j}\left(\bar{\mathbf{W}}_{c,k}^{n+1}\right) \tag{17}$$

Finally, the components of the solution vector $\mathbf{W_k}$ are calculated to deal with the solution of the next time level.

3.3   *The Conservation-Element Solution-Element method*

The CE-SE method [6] solves the governing equations subdividing the space-time mesh into rhombic regions (Solution Element (SE)), in which the solution is provided by Taylor's approximation, and into rectangular regions (Conservation Element (CE)), in which the conservation equations are fulfilled.

The Taylor's approximation applied in every SE, which is centred in a mesh node (j, n), is given by equation (18)

$$w_{k,m}\left(x,t;j,n\right) = \left(\sigma_{k,m}\right)_{j}^{n} + \left(\alpha_{k,m}\right)_{j}^{n}\left(x - x_j\right) + \left(\beta_{k,m}\right)_{j}^{n}\left(t - t^n\right), \tag{18}$$

where:

$$\left(\sigma_{k,m}\right)_{j}^{n} = w_{k,m}\left(x_j, t^n; j, n\right) \tag{19}$$

$$\left(\alpha_{k,m}\right)_{j}^{n} = \frac{\partial w_{k,m}}{\partial x}\left(x_j, t^n; j, n\right) \tag{20}$$

$$(\beta_{k,m})_j^n = \frac{\partial w_{k,m}}{\partial t}(x_j, t^n; j, n) \tag{21}$$

In equations (18)-(21) m takes the value 1 to 3 for the mass, momentum and energy conservation equations respectively.

The conservation laws in every CE are expressed in integral form:

$$\iint\limits_{CE\left(j,n+\frac{1}{2}\right)} \left(\frac{\partial w_{k,m}}{\partial t} + \frac{\partial f_{k,m}}{\partial x}\right) dxdt + \iint\limits_{CE\left(j,n+\frac{1}{2}\right)} (c_{k,m} + c_{w_k,m}) \, dxdt = 0 \tag{22}$$

The first addend of equation (22) can be rewritten as a path integral in the boundary of CE $(j, n+\frac{1}{2})$ applying the Green's theorem [6, 12]. The second addend in equation (22), which accounts for the surface integral corresponding to the source terms (change of area, friction, heat transfer and porous wall), can be approximated from the three SE in which is divided every CE:

$$\iint\limits_{CE\left(j,n+\frac{1}{2}\right)} (c_{k,m} + c_{w_k,m}) \, dxdt = \sum_{l=1}^{3} \iint\limits_{\Omega_l} (c_{k,m} + c_{w_k,m}) \, d\Omega \tag{23}$$

$$\iint\limits_{CE\left(j,n+\frac{1}{2}\right)} (c_{k,m} + c_{w_k,m}) \, dxdt \approx \frac{\Delta x \Delta t}{4} \left[\frac{(c_{k,m})_{j+\frac{1}{2}}^n + (c_{k,m})_{j-\frac{1}{2}}^n}{2} + (c_{k,m})_j^{n+\frac{1}{2}} \right. $$
$$\left. + \frac{(c_{w_k,m})_{j+\frac{1}{2}}^n + (c_{w_k,m})_{j-\frac{1}{2}}^n}{2} + (c_{w_k,m})_j^{n+\frac{1}{2}} \right] \tag{24}$$

The components of the source term vector corresponding to the cross-section area change, friction and heat transfer in a square channel of the wall-flow monolith are written as:

$$c_{k,1} = \sigma_{k,2}\delta_k \tag{25}$$

$$c_{k,2} = \frac{\sigma_{k,2}^2}{\sigma_{k,1}}\delta_k + \frac{F_w \mu_k}{(\alpha - 2w_p k)^2}\frac{\sigma_{k,2}}{\sigma_{k,1}} \tag{26}$$

$$c_{k,3} = \frac{\sigma_{k,2}^2}{\sigma_{k,1}}\left(\gamma\frac{\sigma_{k,3}}{\sigma_{k,2}} - \frac{\gamma-1}{2}\frac{\sigma_{k,2}}{\sigma_{k,1}}\right)\delta_k - \sigma_{k,1}q \tag{27}$$

The source terms related to the porous nature of the inlet and outlet channels of the wall-flow monolith account for the mass and enthalpy flow through the porous walls. These terms are governed by the filtration velocity:

$$c_{w_k,1} = -\,(-1)^k\,\frac{4\sigma_{k,1}u_{w_k}}{\alpha - 2w_p k} \quad , \quad c_{w_k,2} = 0 \quad \text{and} \quad c_{w_k,3} = -\,(-1)^k\,\frac{4h_{0w}\sigma_{k,1}u_{w_k}}{\alpha - 2w_p k} \quad (28)$$

In order to reduce the computational cost of the CE-SE method, an explicit formulation for the solution of the source terms has been adopted according to the proposal of Briz and Giannattasio [5]. Additionally, the solution of every node (j,n) of an inlet channel is coupled to the solution of the corresponding node (j,n) in the outlet channel because of the calculation procedure of the filtration velocity. As in the case of the Lax&Wendroff method, the filtration velocity has been evaluated in intermediate time-steps and nodes.

4.   Discussion of the results

This section is devoted to assess the performance of the two-step Lax&Wendroff method, combined or not with FCT, and the CE-SE method when solving the governing equations in a pair of inlet and outlet channels of wall-flow DPF monoliths. The evaluation of the numerical methods is based on the performance of the solution in a shock-tube tests adapted to the specific case of wall-flow monolith channels. The simulations are computed assuming perfect gas and the lack of friction, heat transfer and area change.

The approached shock-tube test consists of a pair of inlet and outlet channels. A diaphragm in the inlet channel separates two regions where the flow has different conditions in pressure and temperature. An additional diaphragm is placed on the porous wall so that source terms due to porous medium flow are inhibited. The flow conditions in the outlet channel are equal to those in right side of the inlet channel.

The separation between both flow regions in the inlet channel is imposed in the centre of the domain defined as $D = \{x : x \in [-1,1]\}$ m, which is expressed in meters. This diaphragm and the one which is placed on the porous wall are removed at time $t = 0$ s. The initial conditions in every region are detailed in Table 1, which are representative of the beginning of the DPF operation during an engine start, both in magnitude of pressure and temperature discontinuity. The inlet and outlet channels have a honeycomb cell size of 1.486 mm. The porous wall has 0.3 mm in thickness and the wall permeability is $2.49x10^{-}13$ m^2.

Figure 3 shows the evolution in time of the flow properties in the inlet and outlet channels obtained with the CE-SE method and a spatial mesh size of 0.66 mm. The solution provided by the CE-SE method with this mesh is taken as reference because of the lack of exact solution for the proposed shock-tube test and the accuracy of this method when applied to shock waves problems in 1D problems [22, 23]. The continuous line represents the solution in the inlet channel and the dashed line refers to the outlet channel flow properties.

When the diaphragms are removed, a mass flow is instantaneously established across the left side of the porous wall because of the difference in pressure between the left side of the inlet channel and the outlet channel. This is the reason of the positive filtration velocity (from inlet to outlet channel) at time 0.0001 s in the domain $\{x : x \in [-1, -0.054]\}$ m. A region of negative filtration velocity appears at this time in the domain $\{x : x \in [-0.054, -0.017]\}$ m. This domain defines the region of the rarefaction wave. The temperature in this domain is higher in the inlet channel than in the outlet one so that the rarefaction wave, which is mainly dependent on the speed of sound, travels faster in the inlet channel. Consequently,

the pressure becomes higher in the outlet channels producing the back-flow towards the inlet channel.

As time goes by, the pressure in the region of the left side of the channels which has been not reached by the rarefaction wave becomes balanced due to the initial flow across the porous walls. This phenomenon reduces the pressure in the inlet channel increasing it in the outlet one. Additionally, the backward advance of the rarefaction wave produces a region of negative filtration velocity. This region increases in length with time because of the higher distance that this wave travels in the inlet channel. However, the negative filtration velocity is reduced in magnitude because of the balance in pressure between the inlet and outlet channels. Difference in filtration velocity between the inlet and outlet channels is explained by the difference in density, which is in turn given by the difference in temperature.

Besides the rarefaction wave effect, a shock wave is generated in the inlet channel when diaphragms are removed. This shock wave produces a region of greater pressure in the inlet channel than in the outlet one. Therefore, a region of flow from the inlet to the outlet channel is generated after the shock wave covering the domain $\{x : x \in [0, 0.036]\}$ m at time 0.0001 s.

The initial filtration velocity discontinuity produces a pressure discontinuity in the inlet channel of second order effect. The back-flow from the outlet to inlet channel when the rarefaction wave is generated leads to the increase of pressure in the inlet channel producing a new contact discontinuity of lower magnitude. It is detected by the small peak of pressure in the front of the shock wave.

It is worth to note the effect of the filtration velocity on the flow velocity field in both of the channels. In solid walls channel, a shock-tube test like the computed one produces a flat velocity profile between the rarefaction and the shock wave. However, in the case of a wall-flow pair of channels, the velocity profile is only flat between the rarefaction wave and the region of positive filtration velocity. In the case of the inlet channel, there is a decrease of flow velocity in the region of positive filtration velocity due to the loss of mass flow through the porous wall. On the contrary, the outlet channel suffers an increase of mass flow because of the flow going into it from the porous wall, which explains the increase of flow velocity at constant density. Finally, the product of density and velocity sets the specific mass flow profile along the time shown in Figure 3.

Figure 4 shows the comparison of the solution provided at time 0.001 s by the CE-SE and the two-step Lax&Wendroff methods in the inlet channel. The spatial mesh size is 20 mm. As converged solution has been taken that shown in Figure 3, which corresponds to the CE-SE method and a spatial mesh size of 0.66 mm. The

Both of the methods are able to reproduce with good accuracy the flow properties in time and space. Nevertheless, the two-step Lax&Wendroff methods is characterized by a dispersive solution with spurious oscillations around the discontinuities, which is typical in shock-capturing methods of second and higher order.

In the case of the CE-SE method, the solution does not show any kind of oscillations which may lead to divergences in the solution as the spatial mesh size increases. This is the most important advantage of the CE-SE method. However, the solution is diffusive, what avoids the method to reproduce small discontinuities. This effect appears around the contact discontinuity in the solution of the specific mass flow in the inlet channel, which is shown in Figure 4. Both the maximum and minimum peak in specific mass flow due to the change in density and the mass flow across the porous medium are not predicted properly.

An interesting alternative is the combination of the two-step Lax&Wendroff method with the FCT technique. Figure 5 compares the solution in the inlet channel of the two-step Lax&Wendroff with and without its coupling with the FCT

technique. In this case, a Damping and Phoenical formulation has been considered for the smoothing and anti-diffusive operators respectively. A slight worse prediction of the filtration velocity is obtained with respect to the use of the CE-SE method, since some dispersion appears in the region of the contact discontinuity. However, the results allow concluding that the use of the FCT technique provides a very similar solution than the CE-SE method but with the advantage of lower computational cost [18].

Nevertheless, the use of the FCT technique is only worth with a spatial mesh size avoiding the divergence of the solution of the two-step Lax&Wendroff method. This situation is shown in Figure 6, which represents the solution applying a spatial mesh size of 33.3 mm. Only the application of the CE-SE method provides an accurate solution although at the expenses of higher diffusion around the discontinuities. The use of the two-step Lax&Wendroff gives as a result a totally diverged solution being its combination with a FCT technique unable to correct it.

An additional sound consideration regarding the use of the FCT techniques is the selection of the smoothing and the anti-diffusion operators. Figure 7 represents the solution of the filtration velocity in the inlet channel with different combinations of the FCT operators. Only a Damping and Phoenical formulation of the FCT operators corrects properly the non-physical overshoots around the discontinuities. Therefore it is only the combined use of the Damping and Phoenical operators advisable to be applied as solver in wall-flow monolith channels.

A comparison between modelled results and experimental data obtained in an impulse test rig is provided in Figure 8. This facility allows the generation of engine-representative pressure pulses, which can be isolated avoiding interferences from boundary conditions. Therefore, reflected and transmitted pressure pulses generated by the tested device obtained. Characteristics of the impulse test rig and the measurement procedure are described in Ref.[24]. This test is usually applied to assess the acoustic performance of elements in the intake and exhaust lines of internal combustion engines. It is based in the sudden generation of an isolated pressure wave of a given amplitude and duration, which determines the incident pressure wave. The use of experimental data provides added value to the assessment of the adapted numerical methods to the type of 1D systems presented in this paper due to the fact that it gives a proper insight to the problem whose solution is being sought.

Figure 8 shows that the use of any of the adapted methods analysed in this work is able to accurately reproduce the dynamic and the acoustic response of a wall-flow monolith both in time domain and in the frequency domain (sound pressure level (SPL) prediction). Nevertheless, the combination of the two-step Lax&Wendroff method and a FCT technique allows obtaining a better response in the frequency domain because of a prediction of the sound pressure level (SPL) without noise although with a slight drift of the transmitted and reflected SPL as the frequency increases. Negligible differences have been found comparing with the CE-SE method results.

5. Conclusions

The use of shock capturing methods to solve unsteady compressible flow in wall-flow diesel particulate filters provides good accuracy in the prediction of pressure drop, heat transfer and acoustic performance. However, the solution of inlet and outlet channels is coupled because of the source terms in the governing equations which are dependent on the porous wall permeability and the flow properties in every channel. This paper has described in detail the adaptation of the two-step

Lax&Wendroff method and the CE-SE method in order to be applied to the solution of the governing equations in this kind of 1D structures.

A shock-tube test has been proposed to assess the performance of every of the involved methods. The two-step Lax&Wendroff method shows the typical spurious oscillations around discontinuities generated by second or higher order symmetric schemes. The combination of the two-step Lax&Wendroff method and a FCT technique contributes to remove these oscillations. However, this coupling is very dependent on the formulation of the diffusion and anti-diffusion operators. The results in this work show that only the combination of a Damping diffusion and a Phoenical anti-diffusion operators provides accurate results. Similar results to the two-step Lax&Wendroff method with FCT technique are obtained applying the CE-SE method, although at the expense of an increase of the computational effort. However, this drawback may be compensated by the lower sensibility of the CE-SE method to a mesh size increase, which has been shown to be critical when the two-step Lax&Wendroff method is used. Finally, the numerical solution of every method has been compared with experimental data obtained in an impulse test rig. The analysis of the results both in the time and the frequency domain has shown the ability of every of the adapted methods to properly reproduce the dynamic wall-flow monolith response.

Acknowledgements

References

[1] V. Bermúdez, J.R. Serrano, P. Piqueras, and O. García-Afonso, *Assessment by means of gas dynamic modelling of a pre-turbo diesel particulate filter configuration in a turbocharged HSDI Diesel engine under full-load transient operation*, Proceedings of the Institution of Mechanical Engineers, Part D: Journal of Automobile Engineering 225 (9) (2011), pp. 1134–1155.

[2] V. Bermúdez, J.R. Serrano, P. Piqueras, and O. García-Afonso, *Analysis of heavy-duty turbocharged Diesel engine response under cold transient operation with a pre-turbo aftertreatment exhaust manifold configuration*, International Journal of Engine Research doi: 10.1177/1468087412457670 (2012).

[3] D. Book and J. Boris, *Flux-Corrected Transport, II. Generalisations of the method*, Journal of Computational Physics 18 (1975), pp. 248–283.

[4] J. Boris and D. Book, *Flux-Corrected Transport, I. SHASTA, a fluid transport algorithm that works*, Journal of Computational Physics 11 (1973), pp. 38–69.

[5] G. Briz and P. Giannattasio, *Applicazione dello schema numerico Conservation Element - Solution Element al calcolo del flusso intazionario nei condotti dei motori a C.I.*, in *Proc. 48th ATI National Congress*, in Italian, 1993, pp. 233–247.

[6] S. Chang and W. To, *A new numerical framework for solving conservation laws – The method of space-time Conservation Element and Solution Element*, NASA Technical Memorandum 104495 (1991).

[7] J.M. Desantes, J.R. Serrano, F.J. Arnau, and P. Piqueras, *Derivation of the method of characteristics for the fluid dynamic solution of flow advection along porous wall channels*, Applied Mathematical Modelling 36 (2012), pp. 3134–3152.

[8] J. Galindo, J.R. Serrano, F.J. Arnau, and P. Piqueras, *Description of a Semi-Independent Time Discretization methodology for a one-dimensional gas dyanmics model*, Journal of Engineering for Gas Turbines and Power 131 (2009), p. 034504.

[9] J. Galindo, J.R. Serrano, P. Piqueras, and O. García-Afonso, *Heat transfer modelling in honeycomb wall-flow diesel particulate filters*, Energy 43 (2012), pp. 201–2013.

[10] L. Gascón, *Estudio de esquemas en diferencias finitas para el cálculo del flujo compresible, unidimensional, no estacionario y no isoentrópico*, Ph.D. thesis, Universitat Politècnica de València (1995).

[11] T. Ikeda and T. Nakagawa, *On the SHASTA FCT algorithm for the equation $(\partial \rho / \partial t) + [\partial (v(\rho)\rho)/\partial x] = 0$*, Mathematics of Computation 33 (1979), pp. 1157–1169.

[12] W. Kaplan, *Advanced Calculus*, chap. §5.5 Green's Theorem, Reading, MA: Addison-Wesley (1991).

[13] P. Lax and B. Wendroff, *Systems of conservation laws*, Communications on Pure and Applied Mathematics 17 (1964), pp. 381–398.

[14] J. Liu, N. Schorn, C. Schernus, and L. Peng, *Comparison studies on the method of characteristics and finite difference methods for one-dimensional gas flow through IC engine manifold*, in *SAE Technical Paper 960078*, 1996.

[15] H. Niessner and T. Bulaty, *A family of flux-correction methods to avoid overshoot occurring with solutions of unsteady flow problems*, Proceedings of the GAMM Conference of Numerical Methods of Fluid Mechanics (1981), pp. 241–50.

[16] F. Piscaglia and G. Ferrari, *A novel 1D approach for the simulation of unsteady reacting flows in diesel exhaust after-treatment systems*, Energy 34 (2009), pp. 2051–2062.

[17] M. Schejbal, J. Stepanek, M. Marek, P. Kocia, and M. Kubicek, *Modelling of soot oxidation by NO_2 in various types of diesel particulate filters*, Fuel 89 (2010), pp. 2365–2375.

[18] J.R. Serrano, F.J. Arnau, P. Piqueras, A. Onorati, and G. Montenegro, *1D gas dynamic modelling of mass conservation in engine duct systems with thermal contact discontinuities*, Mathematical and Computer Modelling 49 (2009), pp. 1078–1088.

[19] J.R. Serrano, H. Climent, P. Piqueras, and O. García-Afonso, *Analysis of shock capturing methods for chemical species transport in unsteady compressible flow*, Mathematical and Computer Modelling doi:10.1016/j.mcm.2011.11.026 (2012).

[20] A.J. Torregrosa, J.R. Serrano, F.J. Arnau, and P. Piqueras, *A fluid dynamic model for unsteady compressible flow in wall-flow diesel particulate filters*, Energy 36 (2011), pp. 671–684.

[21] D. Winterbone and R. Pearson, *Theory of engine manifold design: wave action methods for IC engines*, Professional Engineering Publishing (2000).

[22] X.Y. Wang, C.Y. Chow, and S.C. Chang, *Application of the space-time conservation element and solution element method to shock-tube problem*, NASA TM- 106806, 1994.

[23] X.Y. Wang, S.C. Chang, and P.C.E. Jorgenson, *Accuracy Study of the Space-Time CE/SE Method for Computational Aeroacoustics Problems Involving Shock Waves*, in *38th Aerospace Science Meeting & Exhibit, AIAA-2000-0474*, 2000.

[24] F. Payri, J.M. Desantes, and A. Broatch, *Modified impulse method for the measurement of the frequency response of acoustic filters to weakly nonlinear transient excitations*, Journal of the Acoustical Society of America 107(2) (2000), pp. 731–738.

Table 1. Initial conditions at inlet and outlet channel.

Property	Inlet channel		Outlet channel	
	Left	Right	Left	Right
p [bar]	1.15	1	1	1
T [K]	655	290	290	290
u [m/s]	0	0	0	0

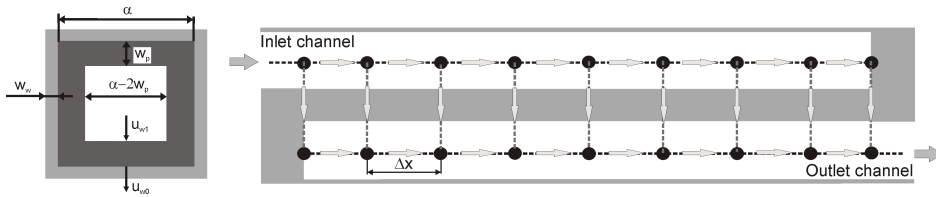Figure 1. Geometry of a pair of inlet and outlet channels of a wall-flow DPF monolith.
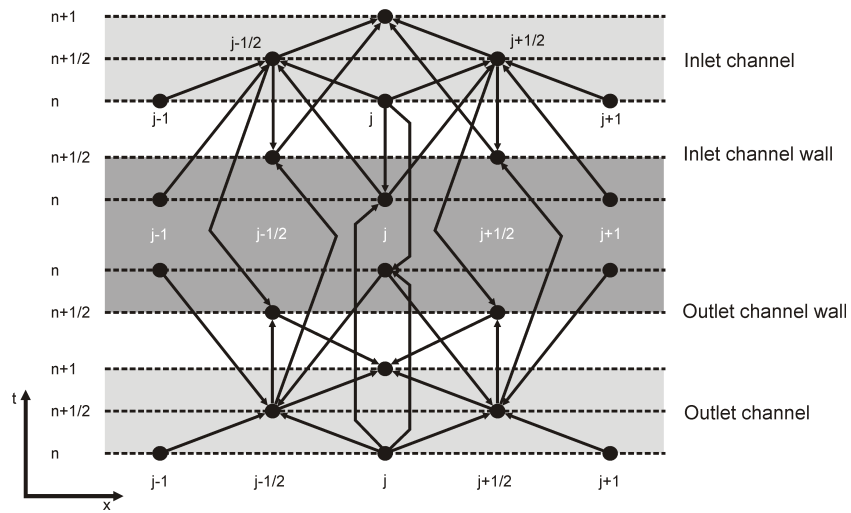
Figure 2.   Computational grid of the two-step Lax&Wendroff method for wall-flow monolith channel solution.
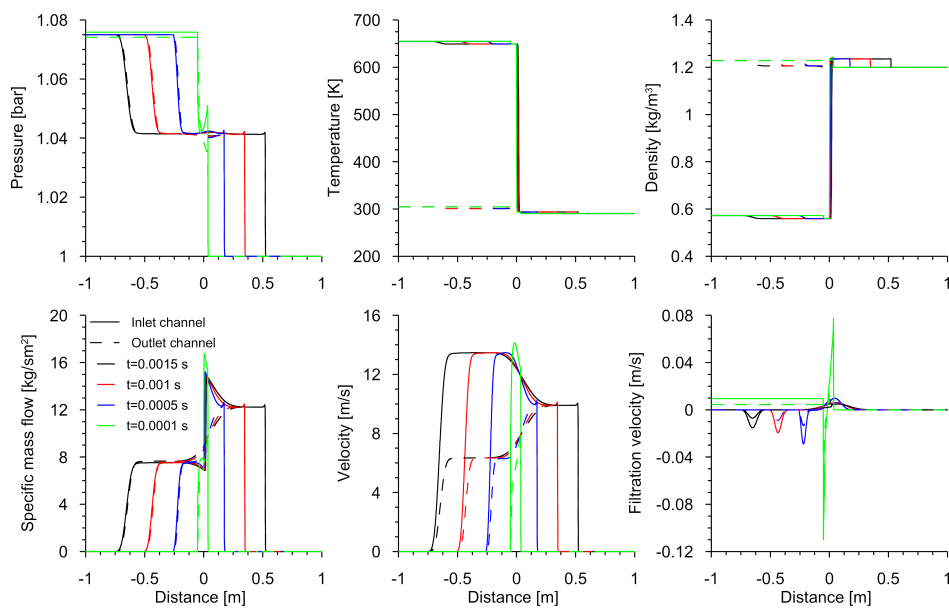

Figure 3.   Shock-tube test solution along the time and space in a pair of inlet and outlet channels with porous walls.
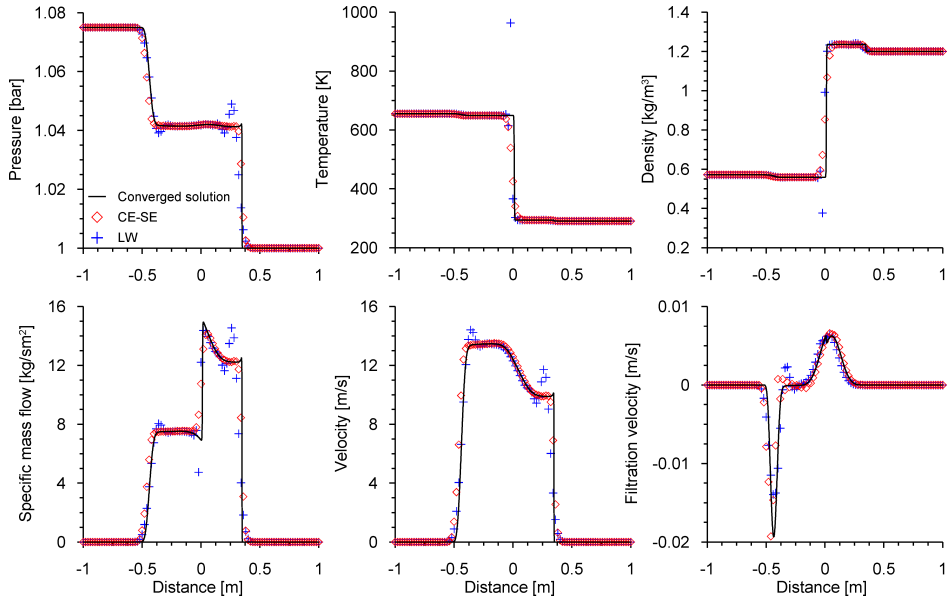
Figure 4.   Comparison between the two-step Lax&Wendroff method and the CE-SE method. Inlet channel properties at time $t = 0.001$ s applying a spatial mesh size of 20 mm.
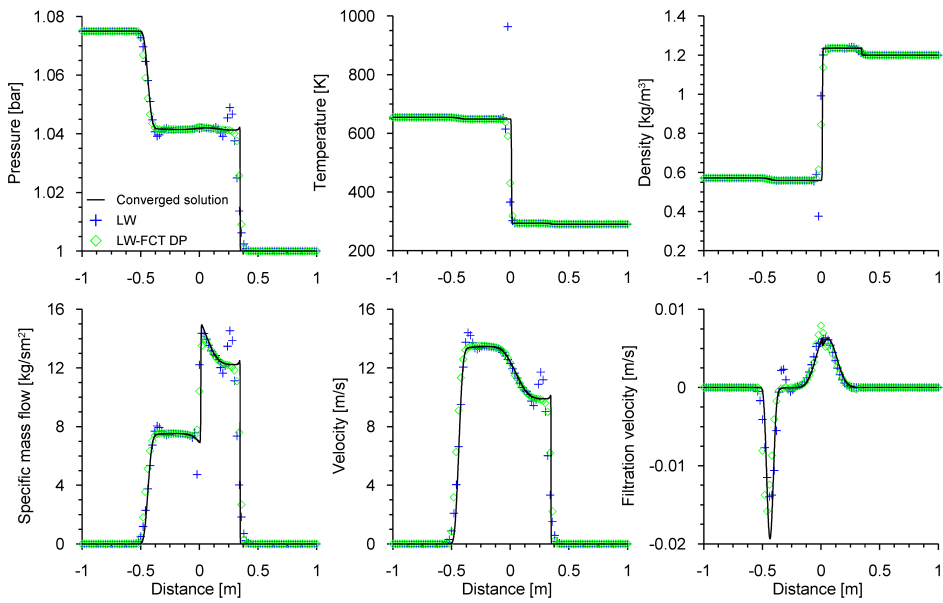

Figure 5.   Comparison between the two-step Lax&Wendroff method and its combination with a FCT technique. Inlet channel properties at time $t = 0.001$ s applying a spatial mesh size of 20 mm.
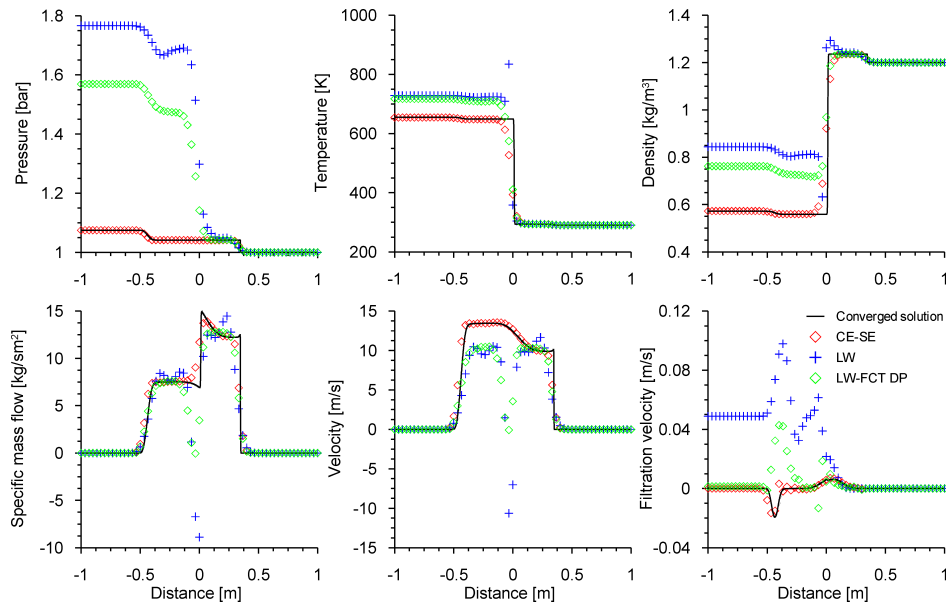
Figure 6. Comparison between the CE-SE method, the two-step Lax&Wendroff method and its combination with a FCT technique. Inlet channel properties at time $t = 0.001$ s applying spatial mesh size of 33.3 mm.
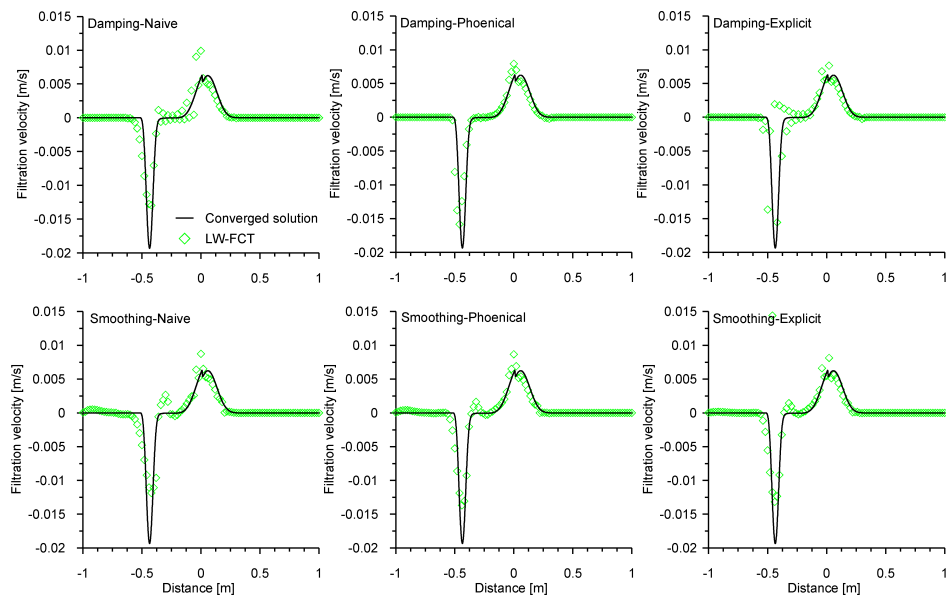

Figure 7. Effect of different FCT operators on the removal of the spurious oscillations generated by the application of the two-step Lax&Wendroff method. Filtration velocity in the inlet channel at time $t = 0.001$ s applying a spatial mesh size of 20 mm.
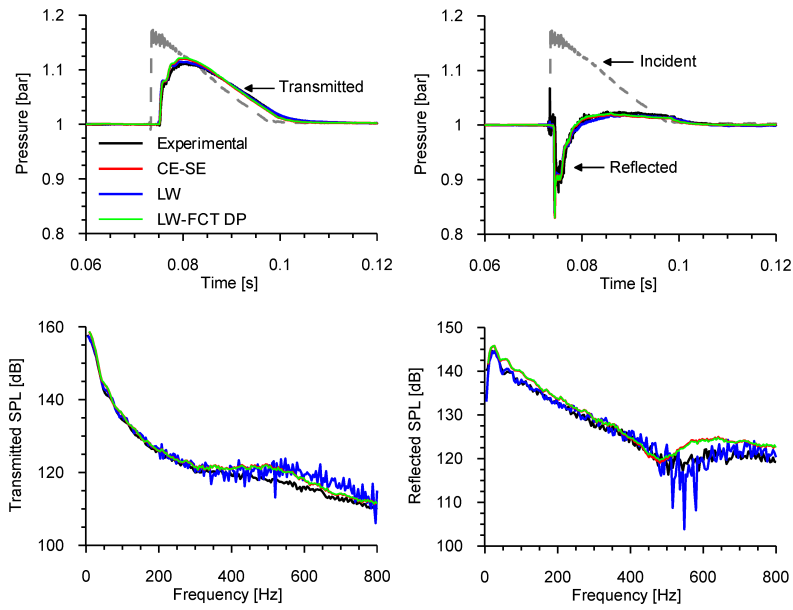
Figure 8.   Comparison between experimental data and modelled results under impulsive flow conditions. Generated pressure pulse of 200 mbar in amplitude and 20 ms in duration.